

Water dynamics inside single-wall carbon nanotubes: NMR observations

Kazuyuki Matsuda,¹ Toshihide Hibi,¹ Hiroaki Kadowaki,¹ Hiromichi Kataura,² and Yutaka Maniwa^{1,3}¹Faculty of Science, Tokyo Metropolitan University, 1-1 Minami-osawa, Hachioji, Tokyo 192-0397, Japan²Nanotechnology Research Institute, National Institute of Advanced Industrial Science and Technology (AIST), 4 Central, 1-1-1 Higashi, Tsukuba, Ibaraki 305-8562, Japan³CREST, JST (Japan Science and Technology Corporation), Japan

(Received 21 June 2006; revised manuscript received 30 July 2006; published 31 August 2006)

The dynamics of water (H₂O and D₂O) molecules adsorbed inside single-wall carbon nanotubes (SWCNTs) of average diameter 13.5 Å were investigated by means of ²H- and ¹H-NMR between 100 and 300 K. Above 220 K, the NMR spectra were substantially narrowed, and indicated that the water is in a liquidlike state with translational and quasifree rotational motions. Below 220 K, where water exhibits long range order inside SWCNTs, the large amplitude molecular motions start to freeze within a time scale of 10⁻⁶ s, while below around 120 K, almost all of the protons become fixed around each atomic site. The results support the dynamic properties and ice-nanotube transition predicted by previous molecular dynamics calculations.

DOI: 10.1103/PhysRevB.74.073415

PACS number(s): 66.30.Pa, 33.25.+k, 64.70.Nd

Single-wall carbon nanotubes (SWCNTs) are able to encapsulate many kinds of materials within their quasi-one-dimensional cavities (ca. diameter of 1 nm).¹ Materials confined within such small cavities are expected to show novel features which do not appear in the bulk material.^{2,3} Water is one such material^{4,5} which can be adsorbed inside SWCNTs in spite of the hydrophobic nature of the SWCNT wall. This water is believed to undergo structural transitions from the liquidlike state to the solidlike state on lowering the temperature (T), to form tubelike structures [so-called ice-nanotubes (ice-NTs)] with long-range order (see Fig. 1).⁴⁻⁶ Furthermore, water exhibits liquid-to-gas-like phase transitions with increasing T .⁵ As illustrated in Fig. 1, there exist several energetically degenerate or nearly degenerate structures in ice-NT structures.⁷ In such cases, the dynamic motion typically associated with protons or water molecules in the liquid state may also be possible in ordered ice-NT structures. However, little is known about the dynamics inside SWCNTs, although limited information has been obtained from NMR and neutron scattering experiments.^{8,9} Here, we report a systematic NMR investigation which explores such dynamics for H₂O/D₂O molecules adsorbed inside high-purity SWCNT samples.

The highly purified SWCNT samples used in the present study were fabricated by laser ablation of Ni/Co-catalyzed carbon,¹⁰ and opened by heating in air for 20–40 min at 350–450 °C. The average SWCNT diameter was 13.5 Å. Samples prepared using essentially the same technique have been characterized by x-ray diffraction (XRD), Raman, and transmission electron microscopy (TEM) observations.^{4,5,11-13} The samples (~20 mg) were set inside quartz NMR tubes connected to a high purity degassed D₂O/H₂O cell. Following evacuation, the sample was exposed to saturated water vapor at room T . XRD experiments on the D₂O samples adsorbed to SWCNTs essentially revealed the same ordering behaviors as the H₂O-adsorbed samples reported previously:⁵ the ordering T of D₂O in SWCNTs is equal to that observed for H₂O samples within 5 K. The NMR experiments were performed in a constant field of 4.0 T using a pulsed Fourier transform NMR tech-

nique with a sequence of 90° pulse followed by a free induction decay signal. The 90° pulse lengths for ¹H and ²H NMR were 1.6 and 14.5 μs, respectively.

Figure 2 shows a series of typical ²H-NMR spectra obtained at different temperatures from 170 to 290 K. It should be noted that no hysteresis was observed between heating and cooling, as confirmed by XRD measurements.⁵ Here, we note three important features: namely a substantially narrowed NMR spectra, a noticeable decrease in NMR intensity at lower temperatures, and the presence of fine structures in the spectra.

First, we discuss full width at half maximum (FWHM) values (<~10 kHz) of the observed ²H NMR spectra, which is much smaller than those obtained (~200 kHz) for static D₂O molecules in bulk ice. Such sharp spectra indicate a narrowing effect, and clearly provide evidence of the existence of the large amplitude molecular motion of water molecules on the NMR time scale estimated by the inverse of static linewidth, i.e., $(2\pi \times 200 \text{ kHz})^{-1} \sim 10^{-6} \text{ s}$. The motional narrowing of the NMR line is a general phenomenon which occurs if the large amplitude molecular motion, with a correlation time shorter than the NMR time scale, can

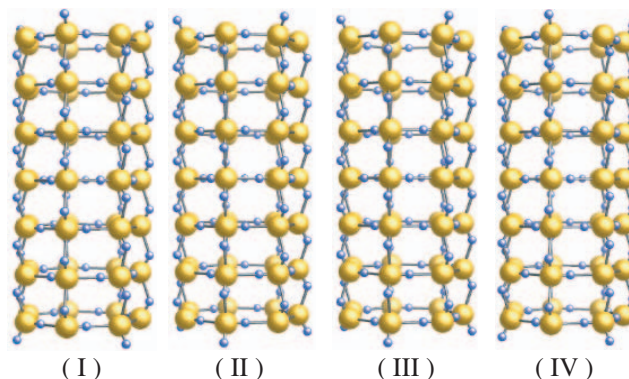


FIG. 1. (Color online) Schematic illustration of the heptagonal ice-NTs with energetically equivalent proton arrangements. Larger spheres represent oxygen atoms and smaller spheres represent hydrogen atoms.

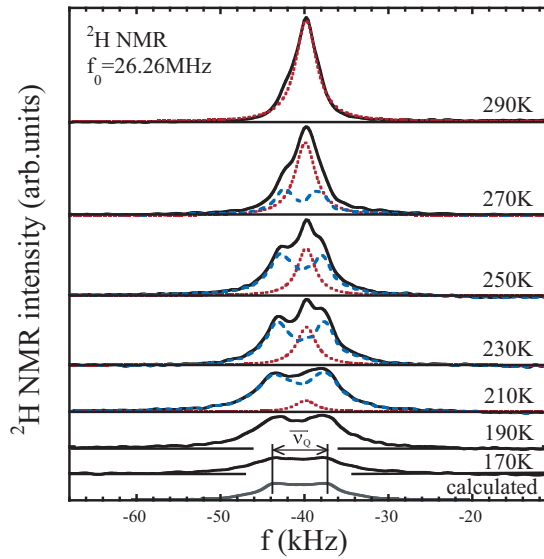


FIG. 2. (Color online) T -evolution of ^2H NMR spectrum for D_2O confined inside SWCNTs. The dotted and dashed lines denote the single-peak and double-peaked components, respectively. The double-peaked components were obtained by subtracting the Lorentzian components from the observed ^2H NMR spectra. A calculated line shape with $\bar{\nu}_Q=6.8$ kHz and $\eta=0$ is also displayed in the figure (bottom). The line shape is convoluted with a Lorentzian function with FWHM of 2.1 kHz.

average out the local field.¹⁴ The ^2H nucleus, which has a spin $I=1$ and a quadrupole moment $Q=2.8 \times 10^{-3}$ b, couples with the local electric field gradient (EFG) tensor V at the site of the ^2H nucleus.¹⁴ As a result, the high field NMR spectrum in randomly oriented D_2O samples exhibits a double-peaked structure. The EFG of D_2O is almost fully determined from the intramolecular properties, affording $V_{zz} \sim 3.1 \times 10^{17}$ V/cm² and $\eta=(V_{yy}-V_{xx})/V_{zz} \sim 0.1$ for the principal values of V , which gives rise to a separation of $\nu_Q \sim 150$ kHz for the double-peaked structure.¹⁵ The observed narrowed spectra imply that the rotational motions of the water molecules must be nearly isotropic in order for them to average out the anisotropy of the EFG tensor within 5% (=10 kHz/200 kHz). A weak deviation from the completely isotropic rotation gives rise to small fine structures as shown in Fig. 2 such that the ^2H NMR spectra cannot be described by a single Lorentzian-type function expected for the ideal isotropic rotation. This, the third important feature, will be discussed later.

The second important point to be discussed is the intensity of the observed ^2H NMR signal. In principle, the integrated spectrum intensity I_S is proportional to the nuclear magnetization, which follows the Curie law under the usual T (>5 mK) and field (a few Tesla) conditions; $\propto N/T$ where N is the number of spins contributing to the signal. Therefore the product, $I_S \times T$, must be constant with T . This is the case above 220 K, as shown in Fig. 3(a). However, below 220 K, the $I_S \times T$ values start to decrease with lowering T , such that some of the NMR signals disappear. Such behaviors indicate NMR line broadening extending over the observation window due to freezing of the molecular rotational motions. This

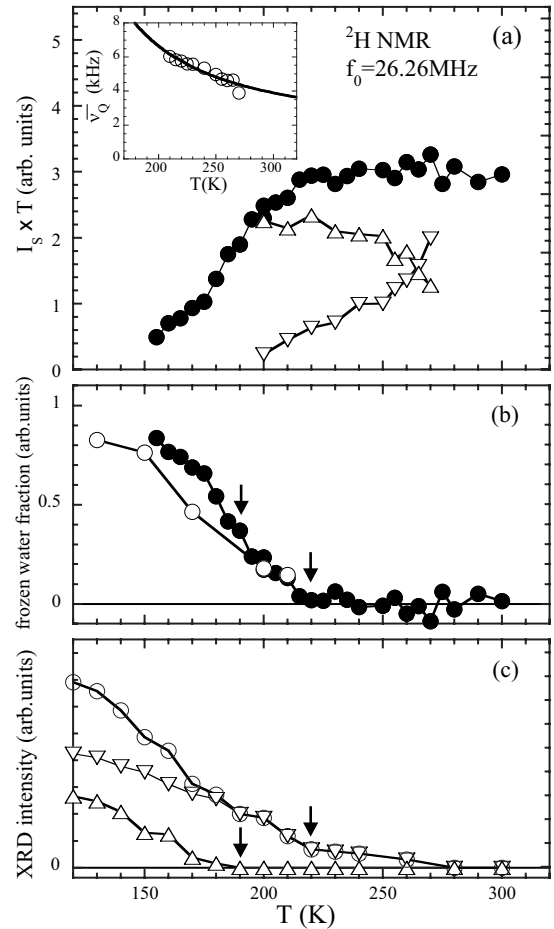


FIG. 3. (a) T -dependence of the ^2H NMR intensity and $T, I_S \times T$ (\bullet) product. The $I_S \times T$ for the single Lorentzian shape (∇) and double-peaked structural (\triangle) components are also plotted in the figure. In the inset, the values of $\bar{\nu}_Q$ obtained from the double-peaked pattern are plotted. (b) T -dependence of the frozen water fraction estimated from ^1H NMR (\circ) and ^2H NMR (\bullet) intensities. (c) T -dependences of the XRD Bragg peak intensity arising from the ordered structures, heptagonal (∇) and octagonal (\triangle) ice-NTs. For comparison with the NMR results, the sum of the Bragg peak intensities (\circ) is also plotted in the figure.

explanation is consistent with the fact that the instrumentally limited observation window (~ 100 kHz in the present measurements) is much smaller than the ^2H -NMR line width for static D_2O molecules ~ 200 kHz. Therefore we conclude that some D_2O molecules lose their rotational mobility below ~ 220 K.

For the SWCNT samples used in the present experiments, the XRD measurements confirm the long range ordered structures assigned to the heptagonal and octagonal ice-NTs below $T_C=225$ and 190 K, respectively. The T -dependences of the Bragg peak (so-called ice-peak) intensity arising from these ordered structures are also shown in Fig. 3(c) for comparison.⁵ It is found that the gradual decrease in the intensity of the NMR signal on cooling is well-correlated with the development of ice-NTs. From this coincidental occurrence, it appears to be quite natural that the reorientational motions of water molecules are frozen in ice-NTs.

Next, we discuss the ^1H NMR spectra taken at several

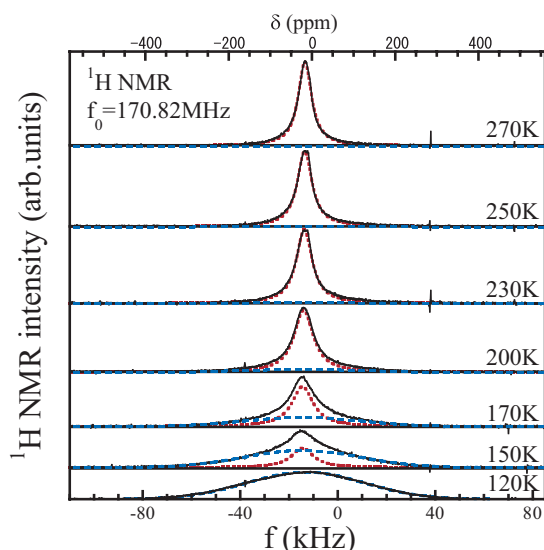


FIG. 4. (Color online) T -evolution of ^1H NMR spectrum for H_2O confined inside SWCNTs. The upper scale indicates the shift (δ) measured relative to bulk water. The right-hand side is described as the downfield region. The dotted and dashed lines denote the Lorentzian and Gaussian components, respectively.

temperatures (Fig. 4). Unlike the ^2H NMR results mentioned previously, there is no decrease in the NMR intensity down to ~ 100 K from 270 K, that is, the ^1H NMR signal arising from the majority of the water molecules in SWCNTs is observable down to 100 K. As seen in Fig. 4, the NMR linewidth increases on cooling from 270 K, while the FWHM becomes almost constant (56 kHz) below ~ 120 K. However, a detailed inspection of the NMR spectra reveals at least two components in the intermediate T -region ($120 < T < 220$ K). As shown in Fig. 4, we found that using a broad Gaussian line with a fixed FWHM (~ 56 kHz) and a sharp Lorentzian line, it was possible to successfully reproduce the observed spectra. Although the relative intensities of the broad and sharp lines contain a large uncertainty, the analysis definitely indicates coexistence with different NMR signals, corresponding to water molecules with different motions. Here, the broad component increases with decreasing T . This interpretation is consistent with the ^2H -NMR results, where the coexistence of a broad NMR signal with $\text{FWHM} > \sim 100$ kHz and a motional-narrowed NMR signal is observed below 220 K. In Figs. 3(b) and 3(c), it is shown that the broad line intensity shows similar T dependence to that of the lost signal for ^2H and the intensity of the Bragg peak (ice-peak) due to the ordered ice. Thus both the broad signals for ^1H and ^2H are ascribed to immobile water in ice-NTs. The results support the molecular dynamics (MD) calculations which indicated that water molecules in ice-NT have the same order of diffusion constant as in bulk ice ($D \sim 10^{-10} \text{cm}^2/\text{s}$).⁶

For further quantitative discussion of the ^1H NMR line at the lowest T , we calculated the ^1H -NMR second moment (M_2) for the rigid ice-NT lattice using Van Vleck's method. For randomly oriented powder samples, the ^1H -NMR second moment owing to ^1H - ^1H dipolar interactions is given by

$$M_2 = \frac{3}{5} \left(\frac{1}{2\pi} \right)^2 g^2 h^2 I(I+1) \sum_i r_{ij}^{-6},$$

where r_{ij} is the distance between nuclei, g the gyromagnetic ratio, I the spin quantum number (in this case, $I=1/2$), and h Planck's constant.^{14,16} Using the structures for heptagonal and octagonal ice-NTs,⁵⁻⁷ we obtained $M_2=435.3$ and 425.9 kHz.² Accordingly, the $\text{FWHM}_{\text{cal}} (=2.36\sqrt{M_2})$ values for the heptagonal and octagonal ice-NTs are 49.1 kHz and 48.6 kHz, respectively, on an assumption of a Gaussian-shaped resonance line.

Certainly, the ^1H NMR spectrum taken at 120 K can be well fitted by a Gaussian function, as shown in Fig. 4, and the experimental value (~ 56 kHz) for the FWHM agrees very well with that calculated above for the rigid lattice. This fact indicates that all of the protons are essentially frozen at this T , although several structures related to the proton arrangement in ice-NT structures are energetically degenerate or nearly degenerate,⁷ as exemplified in Fig. 1. Therefore it is presumed that the potential barriers for the cooperative proton transfers among the degenerate and nearly degenerate structures are much larger than ~ 100 K.

Now, we discuss the disordered phase above 220 K. As already mentioned, the ^2H NMR spectra reveal that the confined water molecules exhibit rapid rotational motion. However, information regarding the translational motion of these molecules is precluded, because ^2H -NMR spectra only really reveal information regarding the intramolecular properties. Here, we discuss the translational motion in terms of the ^1H NMR spectra. Let us consider a simple case where the water molecules rotate isotropically at fixed points, while keeping the oxygen sublattice of the ice-NT (as a model for frozen translational motion). The rapid, isotropic rotational motion of the water molecules averages the intramolecular ^1H - ^1H dipolar interaction essentially to zero. Therefore the observed ^1H NMR line shape is determined by the intermolecular ^1H - ^1H dipolar interaction, and calculated to be $\text{FWHM}_{\text{cal}} = 24$ kHz. Above 220 K, the experimental linewidth (6–8 kHz) for ^1H NMR is much smaller than 24 kHz for the model of frozen translational motion. Hence translational motion must occur, and causes an additional narrowing of the intermolecular linewidth. This result is consistent with a liquid like state in high T regions, as suggested in the previous MD calculations,⁶ which predicted a diffusion constant of the same order as bulk water in ice-NT ($D \sim 10^{-5} \text{cm}^2/\text{s}$).

The observed ^1H NMR linewidth must also include other contributions such as inhomogeneous broadening due to the anisotropic susceptibility of SWCNTs and the magnetic impurities. These inhomogeneous broadenings (ca. 4 kHz) were estimated from NMR observations of adsorbed gases inside SWCNTs,¹⁷ following the discussion by Kleinhammes *et al.*¹⁸ Deviation from the isotropic molecular rotation also gives rise to a residual intra-dipolar broadening. In the present case, this broadening was estimated as ~ 2 kHz above 220 K from a comparison with the ^2H -NMR results, as discussed below. Therefore the intrinsic ^1H NMR linewidth due to intermolecular interactions must be roughly

1–3 kHz, assuming a Lorentzian line for each of the contributions.

Finally, we focus our discussion on the observed ^2H NMR line shape. As shown in Fig. 2, the ^2H NMR spectrum shows a single sharp line at high T , and then gradually broadens with decreasing T . At low T , the spectra exhibit fine structures ascribed to water molecules with different rotational motions. Here, it should be noted that a motional narrowing can lead to similar line shapes to the observed one when the orientational correlation time for water molecules is comparable to the ^2H NMR linewidth. However, the spectra must be symmetric in this case, and inconsistent with the observed spectra. Thus the spectra at low T can be divided into two qualitatively different components: a Lorentzian-shaped component and a double-peaked structural component.

It is common knowledge that line shapes with similar fine structures are often observed for adsorbed water molecules in such materials as silica glass, zeolites, and biological membranes.^{19–21} The origin can be explained as follows. Since water molecules at the boundary have a preferential orientation owing to the water-adsorbent interaction and water-water interactions, the rotation of adsorbed water molecules cannot be completely isotropic at finite temperatures. Therefore the EFG tensor is not perfectly averaged out and the resulting ^2H NMR spectra appear with a reduced splitting $\bar{\nu}_Q$ ($\ll \nu_Q$). Indeed, the spectrum at 170 K can be reproduced by a calculation using $\bar{\nu}_Q=6.8$ kHz, $\eta=0$, and an orientational correlation time much shorter than 10^{-6} s, as shown in Fig. 3.

At higher temperatures, because the rotational motion becomes more and more isotropic, the $\bar{\nu}_Q$ value decreases and

the line shape changes to a Lorentzian type. The inset image in Fig. 3 shows the T -dependence of $\bar{\nu}_Q$, and a fitting of the observed splitting of the function $\bar{\nu}_Q=\nu_0 \exp(T_0/T)$, where T_0 represents the energy gain for the preferential direction. Here, we obtained $\nu_0 \approx 1.12$ kHz and $T_0 \approx 365$ K ≈ 0.031 eV from the fitting. Interestingly, the obtained T_0 value is very close to the energy for the adsorption of water molecules to the outside of SWCNTs (5,5), which was estimated from first principal calculations.²²

In summary, we have investigated the molecular motions and proton dynamics of water molecules confined within SWCNTs by means of ^1H and ^2H NMR, in a T -range from 100 to 300 K across the so-called ice-NT formation T_C . Above T_C , motionally narrowed NMR spectra are observed due to the mobile water molecules. This fact indicates that the water inside SWCNTs is in a liquid state, where the translational and rotational motions of the water molecules are fast on the NMR time scale of $\sim 10^{-6}$ s. However, on decreasing T , the molecular rotation deviates slightly from the completely isotropic rotation. This phenomenon was explained in terms of the existence of a preferential orientation of water molecules even in the liquid state. Below 220 K, we observed a decrease in ^2H NMR intensity according to the formation of ordered ices; heptagonal and octagonal ice-NTs. All of the protons/deuterons in the ordered ices are fixed around each hydrogen bond or atomic site on the NMR time scale of 10^{-6} s. These results support the dynamic properties predicted by the previous MD calculations.⁶

This work was supported in part by a Grant-in-Aid for Scientific Research by the Ministry of Education, Culture, Sports, Science and Technology of Japan.

-
- ¹S. Iijima and T. Ichihashi, *Nature (London)* **363**, 603 (1993).
²M. M. Calbi, M. W. Cole, S. M. Gatica, M. J. Bojan, and G. Stan, *Rev. Mod. Phys.* **73**, 857 (2001).
³A. C. Dillon, K. M. Jones, T. A. Bekkedahl, C. H. Kiang, D. S. Bethune, and M. J. Heben, *Nature (London)* **386**, 377 (1997).
⁴Y. Maniwa, H. Kataura, M. Abe, S. Suzuki, Y. Achiba, H. Kira, and K. Matsuda, *J. Phys. Soc. Jpn.* **71**, 2863 (2002).
⁵Y. Maniwa, H. Kataura, M. Abe, A. Udaka, S. Suzuki, Y. Achiba, H. Kira, K. Matsuda, H. Kadowaki, and Y. Okabe, *Chem. Phys. Lett.* **401**, 534 (2005).
⁶K. Koga, G. T. Gao, H. Tanaka, and X. C. Zeng, *Nature (London)* **412**, 802 (2001).
⁷K. Koga, R. D. Parra, H. Tanaka, and X. C. Zeng, *J. Chem. Phys.* **113**, 5037 (2000).
⁸S. Ghosh, K. V. Ramanathan, and A. K. Sood, *Europhys. Lett.* **65**, 678 (2004).
⁹A. I. Kolesnikov, J.-M. Zanotti, C.-K. Loong, P. Thiyagarajan, A. P. Moravsky, R. O. Loutfy, and C. J. Burnham, *Phys. Rev. Lett.* **93**, 035503 (2004).
¹⁰A. Thess, R. Lee, P. Nikolaev, H. Dai, P. Petit, J. Robert, C. Xu, Y. H. Lee, S. G. Kim, A. G. Rinzler, D. T. Colbert, G. E. Scuseria, D. Tomanek, J. E. Fischer, and R. E. Smalley, *Science* **273**, 483 (1996).
¹¹H. Kataura, Y. Maniwa, T. Kodama, K. Kikuchi, H. Hirahara, K. Suenaga, S. Iijima, S. Suzuki, Y. Achiba, and W. Kraetschmer, *Synth. Met.* **121**, 1195 (2001).
¹²H. Kataura, Y. Kumazawa, Y. Maniwa, Y. Ohtsuka, R. Sen, S. Suzuki, and Y. Achiba, *Carbon* **38**, 1691 (2000).
¹³H. Kadowaki, A. Nishiyama, K. Matsuda, Y. Maniwa, S. Suzuki, Y. Achiba, and H. Kataura, *J. Phys. Soc. Jpn.* **74**, 2990 (2005).
¹⁴A. Abragam, *Principles of Nuclear Magnetism* (Oxford, London, 1961).
¹⁵P. Waldstein, S. W. Rabideau, and J. A. Jackson, *J. Chem. Phys.* **41**, 3407 (1964).
¹⁶J. H. Van Vleck, *Phys. Rev.* **74**, 1168 (1948).
¹⁷Y. Maniwa *et al.* (unpublished).
¹⁸A. Kleinhammes, S.-H. Mao, X.-J. Yang, X.-P. Tang, H. Shimoda, J. P. Lu, O. Zhou, and Y. Wu, *Phys. Rev. B* **68**, 075418 (2003).
¹⁹D. W. Hwang, A. K. Sinha, C.-Y. Cheng, T.-Y. Yu, and L.-P. Hwang, *J. Phys. Chem.* **105**, 5713 (2001).
²⁰D. Goldfarb, H.-X. Li, and M. E. Davis, *J. Am. Chem. Soc.* **114**, 3690 (1992).
²¹M. Kodama, Y. Kawasaki, H. Aoki, and Y. Furukawa, *Biochim. Biophys. Acta* **1667**, 56 (2004).
²²R. Pati, Y. Zhang, S. K. Nayak, and P. M. Ajayan, *Appl. Phys. Lett.* **81**, 2638 (2002).